

Photofragmentation dynamics of formaldehyde: CO(v,J) distributions as a function of initial rovibronic state and isotopic substitution

Douglas J. Bamford, Stephen V. Filseth, Mary F. Foltz, John W. Hepburn, and C. Bradley Moore

Citation: *The Journal of Chemical Physics* **82**, 3032 (1985); doi: 10.1063/1.448252

View online: <http://dx.doi.org/10.1063/1.448252>

View Table of Contents: <http://scitation.aip.org/content/aip/journal/jcp/82/7?ver=pdfcov>

Published by the **AIP Publishing**

Articles you may be interested in

[D+H2\(v=1, J=1\): Rovibronic state to rovibronic state reaction dynamics](#)

J. Chem. Phys. **92**, 2107 (1990); 10.1063/1.458044

[Rovibronic state to rovibronic state reaction dynamics: O\(3 P\)+HCl\(v=2,J\)→OH\(v',N'\)+Cl\(2 P\)](#)

J. Chem. Phys. **87**, 7341 (1987); 10.1063/1.453328

[Rotational state distributions of H2 and CO following the photofragmentation of formaldehyde](#)

J. Chem. Phys. **84**, 1487 (1986); 10.1063/1.450494

[Photofragmentation dynamics of formaldehyde: H2\(v,J\) distributions](#)

J. Chem. Phys. **83**, 4476 (1985); 10.1063/1.449015

[Photofragmentation dynamics of ketene at 308 nm: Initial vibrational and rotational state distributions of CO product by vacuum UV laserinduced fluorescence](#)

J. Chem. Phys. **83**, 223 (1985); 10.1063/1.449812



Photofragmentation dynamics of formaldehyde: $\text{CO}(v, J)$ distributions as a function of initial rovibronic state and isotopic substitution

Douglas J. Bamford, Stephen V. Filseth,^{a)} Mary F. Foltz, John W. Hepburn,^{b)} and C. Bradley Moore
Department of Chemistry, University of California, Berkeley, California 94720

(Received 18 September 1984; accepted 26 September 1984)

Complete rotational distributions have been obtained for the CO produced following excitation of H_2CO , HDCO , and D_2CO near the S_1 origin. The CO was detected by vacuum ultraviolet laser-induced fluorescence. The distributions show a remarkable amount of rotational excitation, peaking at $J = 42$, 49, and 53 for H_2CO , HDCO , and D_2CO , respectively, with widths of 20–25 J units (FWHM). $\text{CO}(v = 1)$ from H_2CO photolysis has nearly the same rotational distribution as $\text{CO}(v = 0)$. The population of $\text{CO}(v = 1)$ is $14\% \pm 5\%$ as large as the population of $\text{CO}(v = 0)$, in good agreement with earlier measurements. Increased angular momentum of H_2CO is only partially transferred to CO, giving slightly wider rotational distributions without changing the peak value. The rotational distributions are highly nonthermal, showing that energy randomization does not occur during the dissociation event. An approximate range of product impact parameters has been determined. The impact parameters are too large to be accounted for by forces along the directions of the C–H bonds. The hydrogen appears to be most strongly repelled by the charge distribution a fraction of an Å outside the carbon atom of the CO. The distribution of impact parameters and the internal energy of the hydrogen fragment apparently do not change significantly upon isotopic substitution. The absence of population in $\text{CO}(J < 20)$ confirms the identity of $\text{CO}(J > 25)$ as the long-lived intermediate in formaldehyde photodissociation.

I. INTRODUCTION

Complete quantum state resolution of photofragmentation dynamics is now possible. The availability of increasingly more powerful and more monochromatic laser systems allows the experimentalist to prepare molecules in specific initial quantum states and to detect each quantum state of the products of a photodissociation under collision-free conditions. Most work so far has been directed at observation of final state distributions without selection of a single initial quantum state.^{1,2} It is equally important to resolve initial quantum states. Dixon *et al.*³ recently reported the first rovibronic state-selected photodissociation of a polyatomic molecule (water). Simons² has pointed out that the conservation and disposition of angular momentum can often reveal more about the dynamics of fragmentation than can the conservation and disposition of energy. The formaldehyde molecule is seen below to provide a dramatic experimental example of such a photofragmentation. Accurate *ab initio* potential surfaces for photofragmentation dynamics can now be computed.^{4,5} Dynamical theories for polyatomic molecule photodissociation have progressed greatly but still require

simplifying assumptions for computational feasibility.⁶ There is a clear need for theoretical and experimental studies on the same system to provide an accurate benchmark for testing the highest level of theory and computationally more tractable theories.

Formaldehyde is an excellent benchmark for several reasons. Its ultraviolet absorption spectrum is well resolved and well understood; rotational assignments have been made for many vibronic bands.⁷ Thus one can prepare the molecule in a specific rovibronic state with a sufficiently monochromatic tunable ultraviolet light source. The excited molecule is known to internally convert to the ground electronic state and then dissociate in the absence of collisions.⁸ Both total energy and total angular momentum must be conserved throughout the process; however, vibration and rotation are expected to be strongly mixed in vibrationally excited S_0 .⁹ The photofragments, hydrogen^{10,11} and carbon monoxide,¹² can both be detected in low concentrations using currently available laser spectroscopic techniques; thus it is possible to measure their (v, J) distributions. A complete vibrational distribution for CO^{13,14} and a partial vibrational distribution for H_2 ¹⁵ have previously been determined. The translational energy distribution of the photofragments has also been measured.¹⁶ About two-thirds of the $29\,500\text{ cm}^{-1}$ (85 kcal/mol) of available energy is released in translation; CO is nearly all formed in its ground vibrational state; high rotational states of CO have been observed¹⁷; a very

^{a)} Permanent address: Department of Chemistry, York University, Downsview, Ontario M3J 1P3 Canada.

^{b)} Permanent address: Department of Chemistry, University of Waterloo, Waterloo, Ontario N2L 3G1, Canada.

recent complete H₂(v , J) distribution shows substantial vibrational and modest rotational excitation.¹⁸ The formaldehyde potential surface has served as a testing ground for the state-of-the-art in *ab initio* computation. A high, narrow barrier has been found along the reaction coordinate for formation of H₂ + CO.¹⁹ Since the barrier height is near the total energy content of the photoexcited ($\nu \sim 29\,500\text{ cm}^{-1}$) molecule, the distribution of energy in the products is determined almost entirely by dynamics in the repulsive exit valley. The product quantum state distributions reported here should not depend significantly on the dynamics of the formaldehyde molecule and the distribution of energy among its rovibrational coordinates on the H₂CO side of the barrier. This contrasts markedly with dissociations for which there is no repulsion in the exit channel (e.g., H₂CO \rightarrow H + HCO or H₂CCO \rightarrow CH₂ + CO). Much theoretical work has been done on the dynamics of quasibound formaldehyde.^{5,20-22} Accurate potential surfaces for the exit valley of H₂CO \rightarrow H₂ + CO will surely be computed and will allow many dynamical methods to be clearly tested against the experimental distributions.

The existence of a long-lived intermediate state in formaldehyde photochemistry was suggested following infrared spectroscopic observations that low J states of CO appeared after delays of as much as 5 μ s after formaldehyde photolysis and only as the result of collisions.¹³ The lack of chemically reasonable candidates for such a long lived intermediate,^{13,23} and mounting evidence that dissociation occurs collision free,²⁴⁻²⁶ led to the suggestion that the intermediate was not one of H₂CO but rather highly rotationally excited CO.¹⁶ Molecular beam photofragment spectroscopy¹⁶ proved that dissociation occurs collision free. The observation of an unexpectedly high translational velocity,¹⁶ along with calculations showing that the molecule passes through a bent transition state,¹⁹ were also consistent with the hypothesis that rotationally excited CO is the intermediate. The subsequent vacuum ultraviolet (VUV) observation of CO in J states up to 63¹⁷ gave strong support to that suggestion but did not probe states ($J < 25$) overlapping the IR measurements.

In this work the complete rotational distribution of the CO($v = 0$) photofragment as a function of the initial rovibronic state of the H₂CO has been determined using the technique of VUV laser-induced fluorescence. In addition, the CO($v = 1$) rotational distribution for one rovibronic state of H₂CO has been measured, and the effect of isotopic substitution on the rotational distribution has been observed. The distributions measured here provide the final proof that the intermediate is, in fact, CO(v , $J > 25$) and give much detailed information about the dissociation dynamics.

II. EXPERIMENTAL

In order to carry out state-selected photodissociation followed by state-specific product detection, two separate tunable laser systems were needed. The basic idea of the experiment was simple. The (pulsed) photolysis laser was

tuned onto a formaldehyde absorption peak. A short time after the photolysis pulse, the probe laser pulse was fired. The probe was tuned a small fraction of its linewidth each few pulses in order to obtain a fluorescence excitation spectrum. The internal state distribution of the carbon monoxide photofragment was then determined from the relative peak intensities of that spectrum. An overall schematic is given in Fig. 1.

Tunable ultraviolet radiation for the state-selective photolysis of formaldehyde was provided by a commercial system consisting of an excimer laser (Lumonics model TE-861, 10 Hz, 15 ns) operating on XeCl at 308 nm which pumped a dye laser (Lambda-Physik model 2002E). For H₂CO and D₂CO the dye laser was etalon narrowed to 0.09 cm⁻¹ bandwidth and pressure tuned to produce tunable radiation in the 339 nm region (*p*-terphenyl dye). Formaldehyde fluorescence excitation spectra were taken by sending a small portion of the UV beam through a cell filled with 0.1 Torr of H₂CO or D₂CO, as described by Weisshaar.²⁴ Rotational lines in H₂CO were assigned using line lists provided by Ramsay.²⁷ Partial assignments for D₂CO were available from recent molecular beam spectroscopy experiments.²⁸ Spectral purity of the etalon-narrowed light was assured by periodically using a monochromator (Jobin-Yvon model THR-1500, 1.5 m, second order, double-pass, 0.2 cm⁻¹ resolution) to check for the presence of etalon side modes 1.0 cm⁻¹ away from the central frequency. Such side modes were always less than 5% as intense as the central mode. In the case of HDCO, rotational assignments were not available and the laser was operated without an etalon (0.4 cm⁻¹ bandwidth) and grating tuned to maximize the CO signal. In all experiments reported here the UV beam (15 ns pulse duration) was expanded using a telescope consisting of two quartz cylindrical lenses to give a beam size of ~ 15 by 4 mm at the entrance to the photolysis cell, with pulse

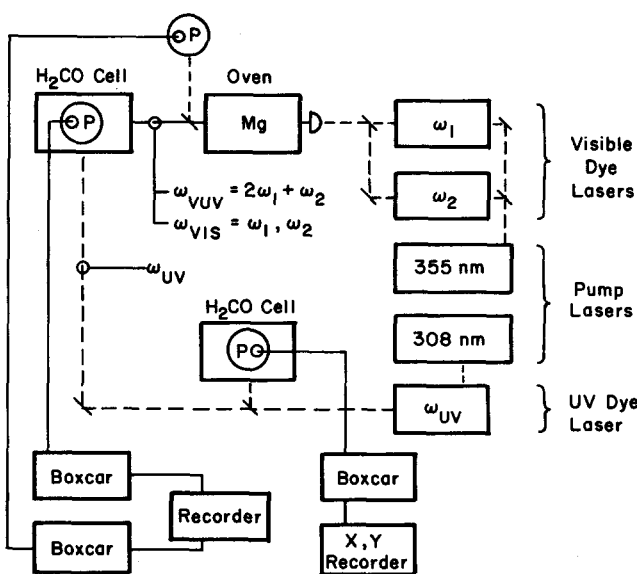


FIG. 1. Schematic drawing of the apparatus for tunable ultraviolet dissociation of formaldehyde followed by vacuum ultraviolet laser-induced fluorescence detection of the carbon monoxide product. Photomultipliers are labeled P.

energies of 2–5 mJ. The beam was double passed through the cell and sent onto a Scientech model 38-0101 power meter for energy monitoring.

The vacuum ultraviolet probe laser system was patterned after the Toronto system described by Hepburn *et al.*²⁹ Frequency-tripled radiation from a Nd:YAG laser (Quanta-Ray DCR-1A) was used to pump two dye lasers. One of these dye lasers (Lambda-Physik model 2002) was fixed at a wavelength of ~ 430.9 nm (Stilbene 420), corresponding to a two-photon resonance in magnesium (ω_1). The other (ω_2) dye laser (Quanta-Ray PDL-1) was tuned between 480–510 nm (Coumarins 480 and 500), or between 565–600 nm (Rhodamine 6G), depending on the band of CO being studied. Energy from each of the two dye lasers was typically 1.0–1.5 mJ per 5 ns pulse within a bandwidth of $0.4\text{--}0.5\text{ cm}^{-1}$. The dye laser beams were combined in a Glan prism, sent through a quarter-wave plate to make them circularly polarized, and focused by a 25 cm focal length glass lens into a magnesium heat pipe oven whose design has been described previously.³⁰ (The dye beams were ~ 3 mm in diameter before being focused.) The oven was operated at $710\text{--}750^\circ\text{C}$, at which magnesium has a vapor pressure of 5–15 Torr.³¹ A mixture of 80 Torr He and 40 Torr Ar was used to protect the oven windows and provide for phase matching. (The amount of VUV radiation generated was relatively insensitive to the exact pressures used.) Gas handling for the oven was carried out using a diffusion-pumped glass and grease vacuum line with a base pressure below 10^{-6} Torr. Tunable VUV radiation ($\omega_3 = 2\omega_1 + \omega_2$) was generated in the focal region of the dye laser beams by resonantly enhanced four-wave mixing.³² The VUV radiation was expected to be circularly polarized in the same sense as the ω_1 laser. The beams exited the oven through a lithium fluoride window and were sent without any collimation into the photolysis cell. A small fraction of the radiation was split off by a lithium fluoride window before the photolysis cell, then spatially dispersed by a sand-blasted copper elbow onto the photocathode of a solar-blind photomultiplier tube (Hamamatsu model 1081) to monitor the VUV intensity. The size of the VUV beam could not be measured directly, but from the size of the visible beams one can estimate that it was ~ 4 mm in diameter in the middle of the photolysis cell. Absolute pulse energies were not measured, but the observed sensitivity for CO detection and the performance of other systems of nearly identical design³³ indicate that there were between 10^{11} and 10^{12} VUV photons in each 5 ns long pulse. The VUV light path was purged with argon to prevent attenuation by air.

The photolysis cell was designed to allow the photolysis and probe beams to cross at right angles. The VUV axis was ~ 30 cm long, with about 12 cm between the entrance to the cell and the interaction region at the intersection of the two beams. The VUV beam entered and exited the cell through MgF₂ windows. The UV axis was ~ 5 cm long, with suprasil quartz windows. The volume of the cell was $\sim 100\text{ cm}^3$. Gas handling was done on a separate glass-and-grease vacuum system with a base pressure below 10^{-6} Torr. Formaldehyde was

delivered into one end of the cell through a stainless steel metering valve and pumped out the other end with a 12 mm diam Teflon stopcock to regulate the pumping speed. The pressure was fixed at 0.05 Torr for all of the CO($v = 0$) spectra and at 0.10 Torr for the CO($v = 1$) spectrum. Pumping speeds of up to 1 l/s with 0.1 Torr of H₂CO in the cell were obtainable. In this way the concentration of thermal CO was kept to a value low enough not to interfere with population measurements.

Formaldehyde was prepared in the usual way.³⁴ Before each experiment, samples were put through two or three freeze–pump–thaw cycles to remove any CO impurities. (Such impurities were readily detected with the VUV system.) Then they were placed in a hexane slush to deliver a vapor pressure of ~ 5 Torr. The Teflon stopcock and metering valve were adjusted to give the desired formaldehyde pressure, as measured by a capacitance manometer (Baratron model 310-BH). The cell pressure was kept constant to within 5% during the course of each experiment.

When carbon monoxide was present in the cell, it could be electronically excited via the $A\ ^1\Pi \leftarrow X\ ^1\Sigma^+$ transition.³⁵ Fluorescence was viewed through a suprasil quartz window on top of the cell. It was collected with a 50 mm diam $f/1$ CaF₂ lens and imaged onto the photocathode of a solar-blind photomultiplier tube (EMR model 542G-09-18). The fluorescence light path was also purged by argon. The quartz window had the virtue of reducing scattered VUV laser light to less than 1 photon per 100 laser shots without any light baffles in the photolysis cell. Thus the absorption by the quartz of more than half of the CO fluorescence could be tolerated. The combination of quartz window transmission and photomultiplier sensitivity produced a detection system with maximum sensitivity at ~ 168 nm and with half-maxima at ~ 163 and ~ 178 nm. The photocurrent from the tube (generally operated at 3 kV with a gain of 10^7) was sent without amplification into a Stanford Research Systems (SRS) model SR 250 gated integrator. In a similar manner, the signal from the Hamamatsu photomultiplier tube used to monitor incident VUV intensity was sent directly to a second SR 250 gated integrator. Both signals were terminated into $50\ \Omega$ and averaged over a 100 ns gate. Triggering was accomplished using a photodiode (EG&G SGD100A) looking at scattered visible laser light. The gated integrator time constants were set at 3 or 10 s (30 or 100 laser shots at 10 Hz).

Fluorescence excitation spectra of CO were generated by sending the outputs of the gated integrators to a 2-pen strip-chart recorder. The wavelength of the ω_2 dye laser was scanned at a linear rate, usually 4–5 gated integrator time constants per laser linewidth. A peak height, $I_{J'}$, could be related to the population in the rotational state of quantum number J'' by the expression

$$I_{J'} \propto (S_{J'J''}/g_{J''})N_{J''}, \quad (1)$$

where $S_{J'J''}$ is the Hönl–London factor of the $J' \leftarrow J''$ transition and $g_{J''} = 2J'' + 1$ is the degeneracy of the state J'' .³⁶ Preliminary spectra were taken by filling the cell with a small partial pressure ($\sim 5 \times 10^{-5}$ Torr) of room

temperature CO. Peak intensities from such spectra, normalized for incident VUV intensity, gave populations which fit to $\pm 5\%$ uncertainty a Boltzmann distribution at a temperature within 5° of room temperature. From the smallest observable peaks in these spectra a detection limit of $\sim 10^8$ molecules per cm^3 per quantum state could be inferred. Based on the widths of resolved peaks, the VUV linewidth was $\sim 1.2 \text{ cm}^{-1}$.

Spectra generated from photochemical CO were analyzed in the same way, although several additional correction factors needed to be applied. (i) Peak heights had to be normalized for changes in incident photolysis laser intensity (as much as a factor of 2 during a single day's experiments because of the short lifetime of the XeCl laser gas mixture). The signal was linearly proportional to UV intensity to within 10% over a factor of 8 range in intensity. Power meter measurements were used to normalize for intensity changes. (ii) Formaldehyde is known to have a broadly structured absorption spectrum in the vacuum ultraviolet,³⁷ and this variable attenuation of the VUV light before it reached the middle of the cell was corrected for by measuring the formaldehyde absorption cross section as a function of VUV wavelength. This was easily done by placing the intensity monitor PMT at the exit of the cell and measuring the amount of VUV attenuation by a known pressure of H₂CO, HDCO, or D₂CO. Cross sections for H₂CO agreed with the earlier lower-resolution measurements of Mentall *et al.*³⁷ to within 10%. No features narrower than the previously observed ones were seen. (The VUV formaldehyde absorption produced a very small amount of background VUV fluorescence. The fluorescence intensity was roughly proportional to the formaldehyde absorption cross section and had a lifetime comparable to the lifetime of fluorescence from the $A^1\Pi$ state of CO. It may have been caused by VUV photodissociation of formaldehyde to form electronically excited CO.) (iii) A third correction had to be applied to account for long-term drift in the signal level during the 3–8 h course of an experiment. This drift was due to a combination of changes in the spatial overlap of the photolysis and probe beams, small changes in the linewidth and wavelength of the photolysis laser, and possibly other factors. The drift was corrected for by periodically (about once an hour) scanning over a set of three reference peaks and assuming linear drift during that hour. Discontinuities caused by retuning of optics and lasers were also corrected for using the reference peaks. The direction of the drift varied from day to day, and sometimes from hour to hour during a single day. It was usually less than 10% per h, and the overall net drift was never more than 30% during a full day. (iv) Small fluctuations in formaldehyde pressure were corrected for by assuming direct proportionality to pressure. (v) A sensitivity correction had to be applied when a complete rotational distribution could not be measured in a single day. The sensitivity correction was made empirically by measuring the populations of several J states on both days. (vi) Finally, the $A^1\Pi$ state of CO is known to be perturbed by lower-lying electronic states. Corrections for strongly perturbed lines were made using mixing coefficients and energy eigenvalues supplied by Field.³⁸

If a line was split by perturbation into two well-resolved transitions, the intensities of the two peaks were added. If only one of the peaks was well resolved, its intensity was divided by the fraction of $A^1\Pi$ character in the upper state of the transition. These correction factors are listed in Tables I and II.

The calculated sensitivity for CO fluorescence detection, based on the estimated spectral response curve of the detection system and known CO emission wavelengths and Franck–Condon factors,³⁹ was constant to within 15% over the entire rotational profile of each CO absorption band used. No correction for J -dependent sensitivity was made.

To produce photochemical CO, the lasers were synchronized by sending the flashlamp synch-out pulse of the Quanta-Ray YAG laser through a variable delay generator which produced two output pulses. One pulse was sent through another variable delay and used to trigger the Q switch of the YAG laser. The other pulse triggered Tektronix 555 oscilloscope whose gate output triggered the excimer laser. The timing of the two lasers was monitored using a photodiode which could see scattered light from both of them. The delay was set for 150 ns in all of the H₂CO and HDCO photolyses, and for 500 ns in the D₂CO photolysis. Jitter amounted to ± 10 ns. The photolysis laser could be tuned onto a formaldehyde absorption as described above or, alternatively, the amount of photochemical CO in a particular J state could be monitored as a function of photolysis laser wavelength. As Fig. 2 shows, the two techniques produced similar spectra. (Differences in relative intensities are expected because of the quantum-state dependence of formaldehyde fluorescence lifetimes.⁴⁰) This confirmed the state-selected nature of the photodissociation, and either technique could be used to locate the formaldehyde absorption lines of interest.

Because the intensity of the laser-induced fluorescence from a photofragment can sometimes depend on the relative polarizations of the photolysis and probe lasers,⁴¹ the intensity of fluorescence from the $Q(40)$ and $R(44)$ transitions in the (2, 0) band of CO was measured as a function of the polarization of the photolysis laser for each of the H₂CO absorption lines used in the experiment. The signal was independent of UV laser polarization to within 10%. For the distributions reported here the pho-

TABLE I. Perturbed CO $A^1\Pi \rightarrow X^1\Sigma^+$ lines leading to two well-resolved transitions.^a

Line	Band	Approximate splitting (cm^{-1})
$P(33)$	(2, 0)	10
$R(38)$	(2, 0)	9
$P(40)$	(2, 0)	9
$R(46)$	(2, 0)	3
$P(48)$	(2, 0)	3
$Q(51)$	(1, 1)	8

^a Reference 38.

TABLE II. Perturbed lines leading to only one well-resolved transition, along with the fraction of $A\ ^1\Pi$ character in the upper state of the clean transition.^a

Line	Band	Fraction of $A\ ^1\Pi$ character ^b
$P(27)a$	(2, 0)	0.91
$R(31)b$	(2, 0)	0.49
$Q(39)b$	(2, 0)	0.46
$Q(25)b$	(2, 0)	0.71
$R(28)a$	(2, 0)	0.82
$Q(42)b$	(2, 0)	0.91
$P(30)b$	(1, 1)	0.67
$R(34)a$	(1, 1)	0.87
$P(27)b$	(1, 1)	0.42

^a The symbols a and b refer to the high and low frequency components, respectively, of a split transition.

^b Reference 38.

tolysis laser was horizontally polarized (i.e., parallel to the direction of propagation of the probe laser).

To test the collision-free nature of the CO rotational distributions, a rotational relaxation experiment was performed. This was done by scanning over a series of six

CO absorption lines corresponding to $J'' = 37\text{--}59$ with several different delay times between the two lasers during a photolysis of HDCO (0.05 Torr). Rotational relaxation would have caused the relative populations of the various J states to change with time. For delay times up to 1.2 μs no such systematic change was seen; the changes in peak heights were smaller than the experimental precision. After 4 μs there was some systematic change, along with an overall decline caused by diffusion of the CO molecules out of the probe laser beam. Thus, rotational relaxation of the high J states of CO formed in this photolysis happens on a timescale at least one order of magnitude slower than the timescale of this experiment, and the distributions are collision free.

The rotational relaxation rate of H₂CO(S_1) by H₂CO, on the other hand, is known to be faster than gas kinetic, with an approximate rate of 50 μs^{-1} Torr⁻¹.⁸ The collisionless decay rates of the H₂CO(S_1) rotational states used in this experiment have been measured to be $\geq 20\ \mu\text{s}^{-1}$.⁴⁰ At 50 mTorr the rotational relaxation rate of 2.5 μs^{-1} will cause quantum number changes for $\leq 13\%$ of the H₂CO(S_1) molecules prior to dissociation.

In the case of D₂CO, the decay rate of the rotational state(s) excited was approximately 0.5 μs^{-1} .²⁸ The 500 ns delay time used therefore limited the amount of rotational relaxation of D₂CO(S_1) by D₂CO. Thus about half of the D₂CO(S_1) which dissociates within the delay time changes rotational quantum state first. No attempt was made to measure the dependence of the CO rotational distribution on the rotational state of the D₂CO.

III. RESULTS

When the desired formaldehyde absorption was located, the VUV probe laser was scanned to obtain the rotational distribution of the CO. Figure 3 shows a portion of a good spectrum. The top trace in Fig. 4 shows

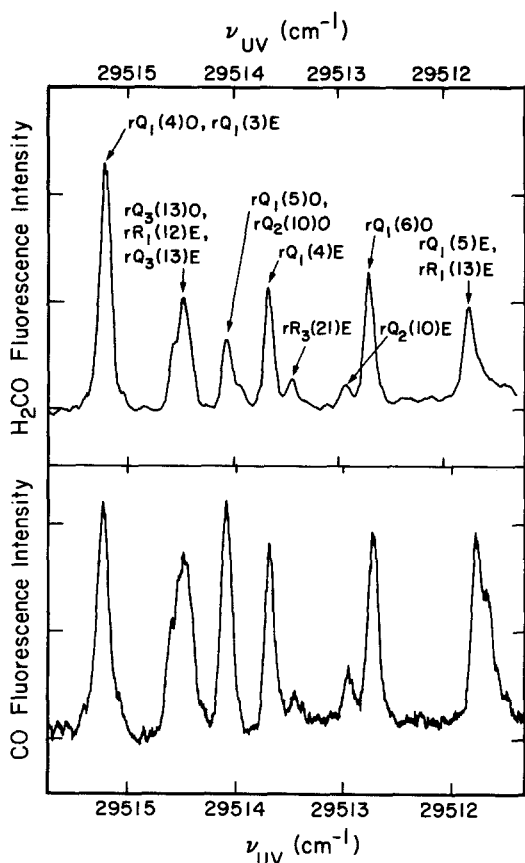


FIG. 2. Two kinds of formaldehyde spectra. The top trace shows the laser-induced fluorescence of 0.10 Torr of H₂CO as a function of photolysis laser wavelength. The bottom trace shows the laser-induced fluorescence signal of CO from the $Q(41)$ transition of the $A\ ^1\Pi \leftarrow X\ ^1\Sigma^+(2, 0)$ band as a function of photolysis laser wavelength (0.05 Torr H₂CO, 150 ns delay between photolysis and probe lasers). Spectral assignments (indicated on the top trace), are the same in both cases, using the notation of Ref. 16. These spectra demonstrate the state-selected nature of the photodissociation. The horizontal scales differ slightly.

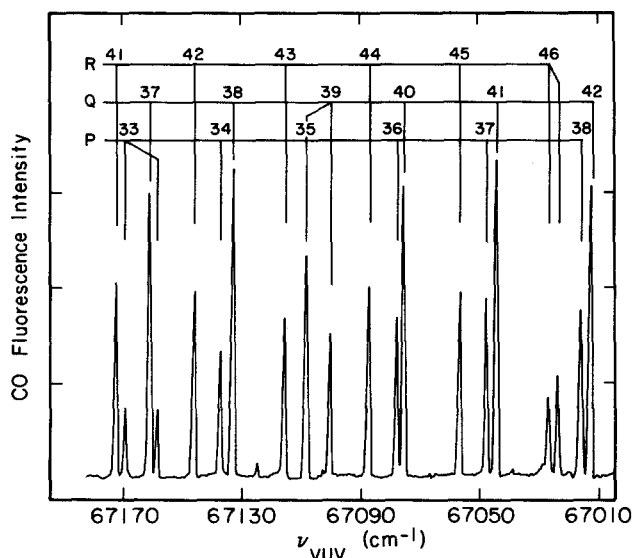


FIG. 3. Portion of a laser-induced fluorescence spectrum of carbon monoxide in the (2, 0) band produced in the photolysis of 0.05 Torr of H₂CO, with the photolysis laser fixed on the $rQ_1(3)E + rQ_1(4)O$ transitions at 29 515.2 cm^{-1} , and 150 ns delay.

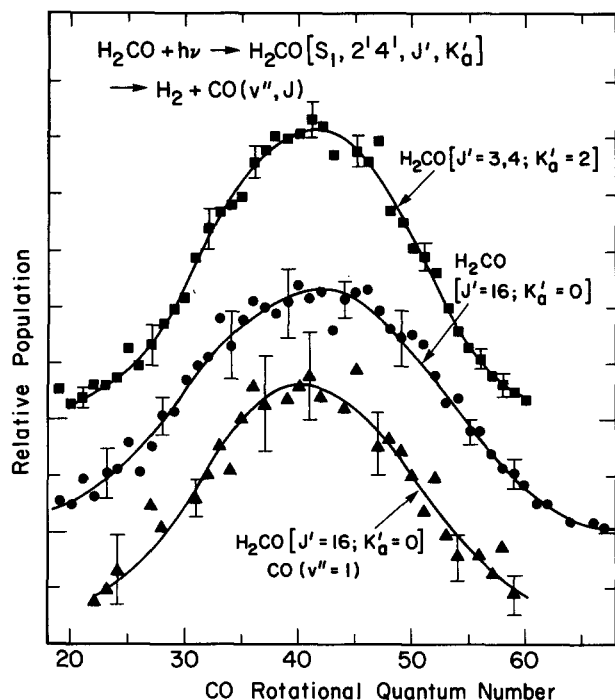


FIG. 4. CO photofragment rotational distributions for H₂CO. Top trace is for CO($v = 0$) produced by photolysis on the $rQ_1(3)E + rQ_1(4)O$ transitions of H₂CO. Pressure was 0.05 Torr and delay 150 ns. Middle trace is for CO($v = 0$) produced by photolysis on the $pR_1(15)O$ transition of H₂CO at 29 490.5 cm⁻¹. Conditions identical to those in the top trace. Bottom trace is for CO($v = 1$) following $pR_1(15)O$ photolysis of 0.10 Torr of H₂CO, with 150 ns delay. The three traces have been displaced by two vertical units. In Figs. 4–6 the curves have all been normalized to the same area, with one vertical unit corresponding to a probability of 0.0178 for formation of a given J state of CO.

the complete rotational distribution for CO($v = 0$) obtained with the photolysis laser fixed on the $rQ_1(3)E + rQ_1(4)O$ transitions at 29 512.2 cm⁻¹ in the 2¹4¹ band of H₂CO. This frequency was chosen because it gives a relatively small amount of angular momentum to the formaldehyde, and is also of interest because it was used in the earlier molecular beam translational energy measurement.¹⁶ Each point is the average of 3–6 experimental peaks. No systematic differences were seen between populations deduced from P , Q , and R lines corresponding to the same J'' , and data from all well-resolved transitions corresponding to a given J'' were averaged together. Error limits represent a spread of ± 1 sample standard deviation from the average, i.e., repeated single measurements would be expected to fall within the limits shown $\sim 65\%$ of the time. The line through the data points is hand drawn and is meant only as a guide to the eye. The distribution has a FWHM of approximately 22 rotational quanta. The rotational distribution of the photolysis laser fixed on the $pR_1(15)O$ line of H₂CO at 29 490.5 cm⁻¹ is shown in the middle trace of Fig. 4. This distribution has a FWHM of ~ 25 rotational quanta. Figure 5 shows the hand-drawn lines through the data for these two photolyses normalized to the same area. The differences between these two rotational distributions are clearly greater than the experimental uncertainty. The total amount of energy available to the molecule is essentially the same in both

cases. The difference between these two photolyses is in the initial angular momentum state of the formaldehyde.

The bottom trace in Fig. 4 shows the rotational distribution for the CO produced in $v = 1$ using the same photolysis line as in the middle trace. This distribution was obtained using the (1, 1) band of CO. Because a different CO $A^1\Pi$ vibrational state was used, this measurement did not directly yield a vibrational distribution for the CO. Based on the estimated spectral response curve of the detection system, and known CO emission wavelengths and Franck–Condon factors,³⁹ the amount produced in $v = 1$ was $14 \pm 5\%$ as large as the amount made in $v = 0$. No signals were seen for CO ($v > 1$).

In order to learn more about the dynamics of the dissociation, experiments were performed on HDCO and D₂CO. The middle trace in Fig. 6 shows the rotational distribution resulting from the photolysis of HDCO at $\sim 29\,515 \pm 2$ cm⁻¹. Because rotational assignments for the 2¹4¹ band of HDCO were not available, the rotational quantum numbers of the state(s) prepared were unknown. The distribution showed no evidence of bimodality. The bottom trace in Fig. 6 shows the distribution for photolysis of D₂CO, also in the 2¹4¹ band. In this case most of the excitation was known to be on the $rQ_0(8)E$ transition at $29\,545 \pm 0.5$ cm⁻¹ from molecular beam experiments.²⁸ However, it was obvious from the room temperature spectrum used to find this transition that the excitation was not clean, and that the contaminating lines must have been due to higher J and/or K states which were not populated in the beam experiments. In the case of both HDCO and D₂CO the effect of isotopic substitution is much bigger than the effect of changing the initial H₂CO rotational state.

IV. DISCUSSION

A. Comparison with earlier work

The results of this experiment mark the final chapter in the history of the “formaldehyde intermediate.” The carbon monoxide is formed with a remarkably high degree of rotational excitation. There is no detectable

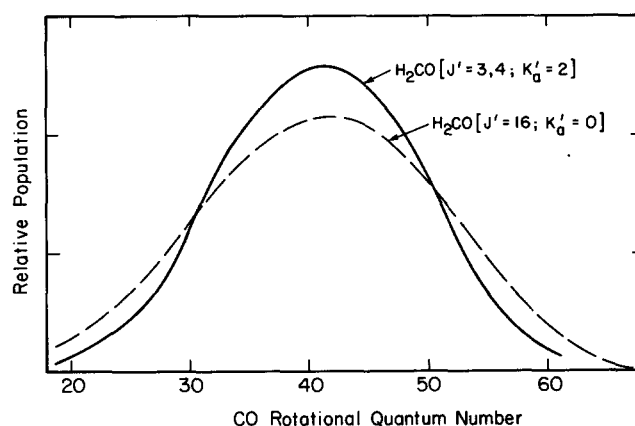


FIG. 5. The effect of initial H₂CO angular momentum on the CO($v = 0, J$) distribution. The hand-drawn lines through the data points in the top two traces of Fig. 4 show a broader distribution for the higher initial angular momentum.

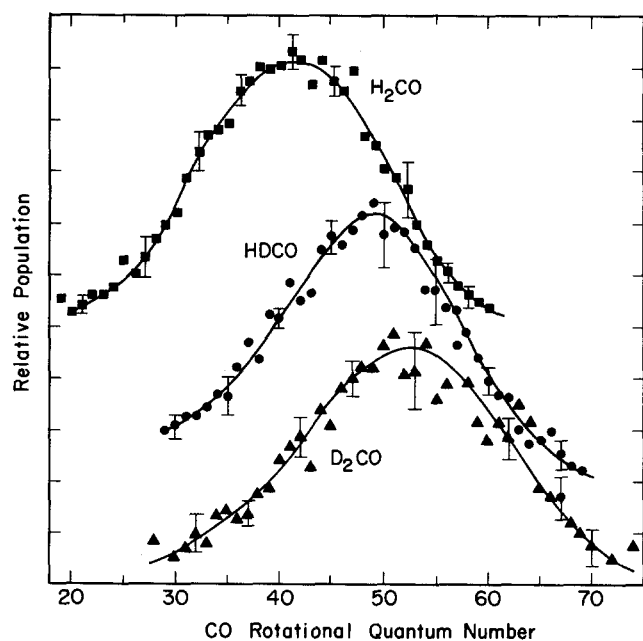


FIG. 6. Effect of isotopic substitution on CO($v = 0$) rotational distributions. Top trace is H₂CO from the top trace in Fig. 4. The middle trace is for HDCO photolysis at $\sim 29\,515\text{ cm}^{-1}$ (0.05 Torr, 150 ns delay). The bottom trace is for D₂CO photolysis at $\sim 29\,545\text{ cm}^{-1}$ (0.05 Torr, 500 ns delay). The middle and top traces have been displaced by two and five vertical units, respectively, from the bottom trace.

population in the J states detected by the earlier CO laser absorption experiments.^{13,14} Rotational relaxation of the high J states formed in the dissociation is slower than gas kinetic, leading to microsecond relaxation times at the lowest pressures (~ 0.1 Torr) used in those experiments. Although no attempt has been made in this work to reproduce the state-specific rise times measured in those experiments, it is clear that the problem was in the interpretation of the results, not the results themselves. The CO formed in $v = 1$ has just as much rotational excitation as that formed in $v = 0$, with more than 90% of the molecules in J states greater than 25. Thus the infrared fluorescence experiments,¹⁴ which were only sensitive to J states below 25, were similarly misinterpreted. These misinterpretations arose out of seemingly reasonable assumptions about rotational relaxation rates and dissociation dynamics. Neither the high translational energy observed in the molecular beam photofragmentation experiment¹⁶ nor the very large impact parameters implied by the present work were anticipated.

A previous experiment using a similar technique has detected CO in J states between 25 and 63 following H₂CO photolysis at 355 nm.¹⁷ J states below 25 could not be observed because of a large thermal CO background. The experiments qualitatively agree in observing high J states of CO, but no detailed comparison can be made because no rotational distribution was reported in that work.

The observed vibrational distribution agrees well with the infrared work: 87% of the molecules in $v = 0$ and 11% in $v = 1$ following H₂CO photolysis at 337 nm.¹³ (The vibrational distributions obtained^{13,14} remain valid because they were obtained under conditions where

rotational relaxation was complete and vibrational relaxation was negligible.)

B. Photodissociation dynamics

A striking aspect of these results is that the energy distributions are strongly nonstatistical. Theories which assume a "statistical" distribution of energy among the vibrational and rotational degrees of freedom of a tetra-atomic (or larger) molecule as it is dissociating generally predict Boltzmann-like rotational distributions for the fragments.⁴²⁻⁴⁴ Figure 7 shows that a temperature cannot be assigned to the observed distributions. The reason for this apparently lies in the steepness of the potential energy surface along the reaction coordinate.¹⁹ After the molecule passes through the energy saddle point on its path to dissociation, the newly forming photofragments experience such a strong repulsion that they fly apart very rapidly, on a timescale shorter than the timescale of vibrational and rotational energy transfers. Therefore, energy is *not* statistically redistributed. (The most probable relative velocity of the photofragments is $1.6 \times 10^6\text{ cm s}^{-1}$,¹⁶ or $1.6\text{ Å}/10^{-14}\text{ s}$.) In a molecule such as HOOH,⁴² CH₂CO,⁴³ or NCNO,⁴⁴ by contrast, the potential energy surface is not significantly repulsive, and all energetically accessible final states appear to be populated with equal probability. The resulting rotational distributions are Boltzmann-like.

It has been suggested¹⁶ that the dissociation can be treated using an impulsive model, collapsing the hydrogen atoms down to a single particle and treating the system as a quasitriatomic. The impulse approximation for non-rotating triatomics has been described by Wilson.⁴⁵ It is known from this work and from earlier infrared experiments^{13,14} that the carbon monoxide has very little vibrational excitation. Thus the version of the triatomic impulse approximation appropriate here is the "modified impulsive model" in which the diatomic has no vibrational excitation and one calculates a ratio of rotational to translational energy using the masses of the three particles and the bond angle of the transition state.⁴⁵ The only approximation involved in such a calculation is the assertion that the final impact parameter b of the particles as they leave each other is determined by the geometry of the transition state. This is based on the chemically

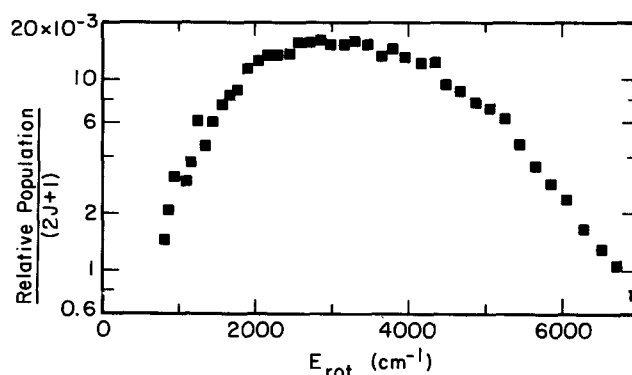


FIG. 7. Boltzmann plot for the data in the top trace of Fig. 4. The distribution cannot be characterized by a temperature.

reasonable assumption that the force applied to the diatomic is applied along the direction of the chemical bond which is being broken. If α is the H₂ "atom" and $\beta\gamma$ is the CO diatomic, the force is applied along the $\alpha\beta$ axis, and the α fragment leaves along that line. Everything else follows from conservation of energy, linear momentum, and angular momentum. The equation which results is⁴⁵

$$E_{\text{rot}} = E_{\text{avl}} \sin^2 \chi / [(m_{\alpha} + m_{\beta})(m_{\beta} + m_{\gamma})/m_{\alpha}m_{\gamma} - \cos^2 \chi], \quad (2)$$

where m_{α} , m_{β} , and m_{γ} are the masses of the three atoms, χ is the bond angle in the transition state, and E_{avl} is the total energy available. The formaldehyde case is more complicated because two bonds are being broken, not one, but a reasonable first approximation would treat the direction of the impulsive force as the vector sum of the directions of the two C–H bonds. This is equivalent to treating the two H atoms as a single particle located at their center of mass. (The fact that HDCO does not yield a bimodal distribution lends support to this approximation.) If this assumption is made and the *ab initio* geometry of the transition state¹⁹ is used, a distribution peaking at $J = 25$ is predicted. Even in the most extreme case, where $\chi = 90^\circ$, the peak shifts only to $J = 35$. To explain distributions for H₂CO photolysis which peak at $J = 42$ and extend out to $J > 60$, the final impact parameter must not be determined by the directions of chemical bonds localized between nuclei. The point of impact must be *outside* the nucleus of the carbon atom.

If the impact parameter b is treated as a variable, not as a quantity determined by the transition state geometry, the conservation laws can be used to relate b to the rotational state of the CO. If the H₂ fragment has no internal excitation and the CO fragment has no vibrational excitation this *exact* equation can be derived⁴⁶:

$$E_{\text{rot}} = E_{\text{avl}} / \{1 + [m_{\beta}m_{\gamma}(m_{\alpha} + m_{\beta} + m_{\gamma})r_{\beta\gamma}^2 / m_{\alpha}(m_{\beta} + m_{\gamma})^2b^2]\}, \quad (3)$$

where $r_{\beta\gamma}$ is the bond length of the $\beta\gamma$ fragment. Using this equation, the peak of the CO rotational distribution at $J \sim 42$ for H₂CO photolysis corresponds to an impact parameter of ~ 0.8 Å, while $J = 60$ corresponds to ~ 1.2 Å and $J = 20$ corresponds to ~ 0.4 Å. Calculations using the corresponding points on the HDCO and D₂CO distributions yield essentially the same results, as shown in Table III.

Now the effect of internal excitation of the hydrogen must be considered. A complete (v , J) distribution for the H₂ will be given in a separate paper.¹⁸ For the purpose of this discussion it can be stated that the maximum values of v and J with appreciable population are 3 and 9, respectively, with the most probable (v , J) state being $v = 1$, $J = 5$. Putting vibrational excitation into the hydrogen has the effect of lowering the value of E_{avl} in Eq. (3). In this case a larger impact parameter (about 0.1 Å for each quantum of H₂ vibration) is needed in order to produce CO in a given J state. Rotational excitation of the hydrogen affects the calculated impact parameter

TABLE III. Calculated impact parameter distributions neglecting energy and angular momentum in H₂.^a

	Calculated impact parameter (Å)		
	H ₂ CO	HDCO	D ₂ CO
Small J_{CO}	0.36 (20)	0.41 (27)	0.39 (29)
Peak J_{CO}	0.79 (42)	0.78 (49)	0.75 (53)
Large J_{CO}	1.2 (60)	1.1 (66)	1.1 (72)

^a The calculations were done with Eq. (3) in the text, using corresponding points on the rotational distributions for photolysis of H₂CO, HDCO, and D₂CO shown in Fig. 6. Small and large J_{CO} are points where the distribution reaches 10% of its peak value. The J_{CO} values are given in parentheses.

in two ways. Conservation of energy causes E_{avl} to be reduced, which slightly increases the value of b that is required to make a given J state of CO. Conservation of angular momentum can raise or lower the impact parameter depending on the direction of the H₂ rotation relative to the direction of the CO rotation. For each J state of CO, a range of possible impact parameters can be calculated using the complete range of possible H₂(v , J) states and J directions. The equation used to do this is derived from the conservation laws (assuming an initially nonrotating formaldehyde molecule).⁴⁷ The minimum possible impact parameters are only slightly lower than those shown in Table III; 0.68 and 1.1 Å for $J = 42$ and $J = 60$, respectively, leaving unchanged the conclusion that the point of impact must be outside the carbon atom. A counter-rotating H₂ can not take up enough angular momentum to lower the impact parameter by more than ~ 0.1 Å. In a separate paper,¹⁸ distribution functions for the impact parameter will be calculated using the complete H₂(v , J) distribution along with the CO(v , J) distributions reported here.

A challenge for theory is to explain these impact parameters—how can they be so large? It is encouraging that the arrows showing motion along the reaction coordinate in *ab initio* calculations⁴ do point the hydrogen fragment in a direction extrapolating to a point of impact outside the carbon atom. It will be important to learn how the directions of the reaction coordinate vectors change as the molecule moves away from the saddle point on its path to dissociation.

Because the hydrogen atoms are not equivalent in the *ab initio* transition state,¹⁹ one might have expected HDCO to yield a bimodal distribution depending on the position of the D atom. The fact that the distribution was not bimodal could mean that the hydrogens come apart from the CO together as a mass 3 unit. Alternatively, in HDCO dissociation could occur from only one of the two possible transition state geometries. In both deuterated species the rotational distributions shift to higher J in a manner quantitatively consistent with the assertion that the distribution of product impact parameters and the internal energy of the hydrogen fragment do not change upon isotopic substitution (see Table III). The increased rotational energy of CO is balanced by a decrease in translational energy in a predictable way, simply because of the change in mass.

The effect of the initial formaldehyde rotational state is modest. A molecule in $J = 16$, $K = 0$ can have up to 16 units of angular momentum about the c axis (perpendicular to the plane of the molecule). *Ab initio* calculations have shown that the molecule remains planar as it moves along the reaction coordinate.⁴ The dissociation event must conserve angular momentum. Because J_{CO} is much larger than J_{H_2} and $J_{\text{H}_2\text{CO}}$, the angular momentum of the CO and the orbital angular momentum of the fragments must be of comparable magnitude and in opposite directions (see Fig. 8). The CO must thus be rotating in one particular sense about the c axis. Since the H₂CO can be rotating in either direction about the axis, its angular momentum can either add to or subtract from the CO angular momentum. At least two factors dilute this effect. First, the angular momentum vector of a near-prolate symmetric top such as H₂CO with $K = 0$ can lie anywhere in the bc plane so that, on the average, only ~ 8 units are available to add directly to the CO angular momentum. (Because $J_{\text{CO}} \gg J_{\text{H}_2\text{CO}}$, components of the H₂CO angular momentum orthogonal to the c axis will not change J_{CO} significantly.) A second effect arises if dissociation is rapid. To visualize this effect, the system can be thought of as a rigid, linear "triatomic" composed of the H₂ atom and the CO diatomic, with a specific angular velocity. Sudden dissociation of this rigid molecule will leave the angular velocity of the diatomic equal to the original angular velocity of the triatomic. The angular momentum of the diatomic will be less than that of the triatomic because its moment of inertia is smaller. In this classical limit the fractional decrease in angular momentum is given by the ratio B/C , where C is the rotational constant of H₂CO about the c axis and B is the rotational constant of CO.⁴⁸ Using the calculated transition state geometry,¹⁹ this ratio is approximately two. From these two effects one would expect that the FWHM of the CO rotational distribution from H₂CO($J = 16$) would be $\sim 6 J$ units greater than the FWHM of the distribution from H₂CO($J = 4$). From Fig. 5, the observed change is $\sim 3 J$ units (FWHM). The remaining factor of two loss in angular momentum cannot be explained by lengthening the C–H bond distances in the transition state. The bond distances would have to be unreasonably long, more than 3 Å, to increase

the moment of inertia by another factor of 2. Apparently some other factor in the dissociation dynamics causes the angular momentum transfer from H₂CO to CO to be less than given by the simplest model.

V. CONCLUSIONS

This experiment has yielded much detailed information about the dynamics of formaldehyde photodissociation. The carbon monoxide fragment has a remarkable amount of rotational excitation. The observed rotational distributions have allowed limitations on the distribution of fragment impact parameters to be determined. The bent transition state geometry predicted by theory¹⁹ has been confirmed. The impact parameters needed to explain the high rotational states of CO seen here are too large to be determined by the directions of the C–H bonds. The hydrogen appears to be most strongly repelled by the charge distribution a fraction of an Å outside the carbon atom of the CO. The nonthermal CO rotational distribution is dynamically controlled; energy randomization does not occur during the dissociation event. The distribution of impact parameters and the internal energy of the hydrogen fragment apparently do not change significantly upon isotopic substitution. CO produced in $v = 1$ has nearly the same rotational distribution as that made in $v = 0$. The initial angular momentum of the formaldehyde is only partially transferred to the carbon monoxide.

The results of this experiment, along with complementary experiments which have measured the translational energy distribution of the fragments¹⁶ and the internal energy distribution of the hydrogen fragment,^{15,18} have led to a nearly complete experimental characterization of the dynamics of this unimolecular reaction. One can hope that theory will be able to deal with the aspects of the dynamics which cannot be probed with the current generation of experiments, e.g., possible correlations between the (v, J) states of the two products and the vectorial relation between the two product angular momenta. At the same time, the results reported here and in the complementary papers will provide the best possible test for theoretical calculations of the formaldehyde potential energy surface, and for theories of reaction dynamics on that surface.

ACKNOWLEDGMENTS

We are grateful to D. A. Ramsay and R. W. Field for providing detailed spectroscopic information on H₂CO and CO, respectively. Some of the laser equipment used in this work was borrowed from the San Francisco Laser Center, supported by the National Science Foundation, NSF Grant No. CHE79-16250, and the National Institutes of Health, NIH Grant No. P41 RR01613-0, awarded to the University of California at Berkeley in collaboration with Stanford University. We are grateful to the U.S. Army Research Office, Research Triangle Park, NC for support of this work. D.J.B. thanks the National Science Foundation for a predoctoral fellowship. J.W.H. thanks NSERC (Canada) for a NATO postdoctoral fellowship.

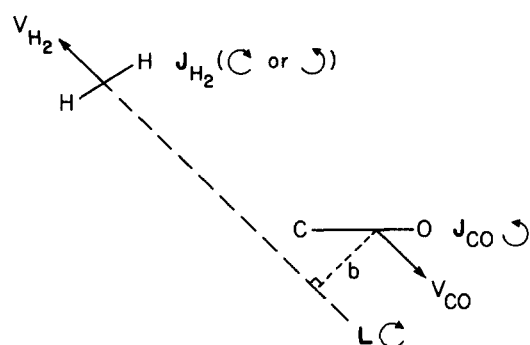


FIG. 8. Diagram showing the relationship between the angular momentum vectors of the two fragments and the orbital angular momentum L of the system as the fragments move apart with velocities v_{CO} and v_{H_2} . A planar dissociation geometry and an initially nonrotating H₂CO have been assumed.

- ¹ S. R. Leone, *Adv. Chem. Phys.* **50**, 255 (1982).
- ² J. P. Simons, *J. Phys. Chem.* **88**, 1287 (1984).
- ³ A. Hodgson, J. P. Simons, M. N. R. Ashfold, J. M. Bayley, and R. N. Dixon, *Chem. Phys. Lett.* **107**, 1 (1984).
- ⁴ J. D. Goddard, Y. Yamaguchi, and H. F. Schaefer III, *J. Chem. Phys.* **75**, 3459 (1981).
- ⁵ S. K. Gray, W. H. Miller, Y. Yamaguchi, and H. F. Schaefer III, *J. Am. Chem. Soc.* **103**, 1900 (1981).
- ⁶ M. Shapiro and R. Bersohn, *Annu. Rev. Phys. Chem.* **33**, 409 (1982), and references therein.
- ⁷ D. J. Clouthier and D. A. Ramsay, *Annu. Rev. Phys. Chem.* **34**, 31 (1983), and references therein.
- ⁸ For a general review of formaldehyde photochemistry, see C. B. Moore and J. C. Weisshaar, *Annu. Rev. Phys. Chem.* **34**, 525 (1983).
- ⁹ H.-L. Dai, C. L. Korpa, J. L. Kinsey, and R. W. Field, *J. Chem. Phys.* (submitted).
- ¹⁰ E. E. Marinero, C. T. Rettner, R. N. Zare, and A. H. Kung, *Chem. Phys. Lett.* **95**, 486 (1983); E. E. Marinero, R. Vasudev, and R. N. Zare, *J. Chem. Phys.* **78**, 692 (1983).
- ¹¹ M. Pealat, J.-P. E. Taran, J. Taillet, M. Bacal, and A. M. Bruneteau, *J. Appl. Phys.* **52**, 2687 (1981).
- ¹² J. W. Hepburn, F. J. Northrup, G. L. Ogram, J. C. Polanyi, and J. M. Williamson, *Chem. Phys. Lett.* **85**, 127 (1982).
- ¹³ P. L. Houston and C. B. Moore, *J. Chem. Phys.* **65**, 757 (1976).
- ¹⁴ C.-K. Cheng, P. Ho, C. B. Moore, and M. B. Zughul, *J. Phys. Chem.* **88**, 296 (1984).
- ¹⁵ M. Pealat, D. Debarre, J.-M. Marie, J.-P. E. Taran, A. Tramer, and C. B. Moore, *Chem. Phys. Lett.* **98**, 299 (1983).
- ¹⁶ P. Ho, D. J. Bamford, R. J. Buss, Y. T. Lee, and C. B. Moore, *J. Chem. Phys.* **76**, 3630 (1982).
- ¹⁷ P. Ho and A. V. Smith, *Chem. Phys. Lett.* **90**, 407, (1982).
- ¹⁸ D. Debarre, M. Lefebvre, M. Pealat, J. P.-E. Taran, D. J. Bamford, and C. B. Moore, (in preparation).
- ¹⁹ J. D. Goddard and H. F. Schaefer III, *J. Chem. Phys.* **70**, 5117 (1979).
- ²⁰ W. H. Miller, *J. Am. Chem. Soc.* **101**, 6810 (1979).
- ²¹ B. A. Waite, S. K. Gray, and W. H. Miller, *J. Chem. Phys.* **78**, 259 (1983).
- ²² W. H. Miller, *J. Am. Chem. Soc.* **105**, 216 (1983).
- ²³ W. M. Gelbart, M. L. Elert, and D. F. Heller, *Chem. Rev.* **80**, 403 (1980), and references therein.
- ²⁴ J. C. Weisshaar and C. B. Moore, *J. Chem. Phys.* **70**, 5135 (1979).
- ²⁵ J. C. Weisshaar and C. B. Moore, *J. Chem. Phys.* **72**, 2875 (1980).
- ²⁶ J. C. Weisshaar and C. B. Moore, *J. Chem. Phys.* **72**, 5415 (1980).
- ²⁷ D. A. Ramsay (private communication).
- ²⁸ D. R. Guyer, W. F. Polik, and C. B. Moore (unpublished).
- ²⁹ J. W. Hepburn, D. Klimek, K. Liu, R. G. McDonald, F. J. Northrup, and J. C. Polanyi, *J. Chem. Phys.* **74**, 6226 (1981).
- ³⁰ J. W. Hepburn, Ph.D. dissertation, University of Toronto, 1980.
- ³¹ J. C. Greenbank and B. B. Argent, *Trans. Faraday Soc.* **61**, 655 (1964).
- ³² S. C. Wallace and G. Zdasiuk, *Appl. Phys. Lett.* **28**, 449 (1976).
- ³³ J. W. Hepburn, *Isr. J. Chem.* (in press).
- ³⁴ R. Spence and W. Wild, *J. Chem. Soc. (London)* **1935**, 338.
- ³⁵ J. C. Simons, A. M. Bass, and S. G. Tilford, *Astrophys. J.* **155**, 345 (1969).
- ³⁶ G. Herzberg, *Molecular Spectra and Molecular Structure, Vol. 1. Spectra of Diatomic Molecules* (Van Nostrand Reinhold, New York, 1950).
- ³⁷ J. E. Mentall, E. P. Gentieu, M. Krauss, and D. Neumann, *J. Chem. Phys.* **55**, 5471 (1971).
- ³⁸ R. W. Field (private communication).
- ³⁹ P. H. Krupenie, *The Band Spectrum of Carbon Monoxide*, Natl. Stand. Ref. Data Ser. Natl. Bur. Stand. **5** (1966), and references therein.
- ⁴⁰ D. J. Bamford, Ph.D. thesis, University of California, Berkeley, 1984.
- ⁴¹ C. H. Greene and R. N. Zare, *J. Chem. Phys.* **78**, 6741 (1983).
- ⁴² T. R. Rizzo, C. C. Hayden, and F. F. Crim, *J. Chem. Phys.* **81**, 4501 (1984).
- ⁴³ D. J. Nesbitt, H. Petek, M. F. Foltz, S. V. Filseth, D. J. Bamford, and C. B. Moore (in preparation).
- ⁴⁴ I. Nadler, J. Pfab, H. Reisler, and C. Wittig, *J. Chem. Phys.* **81**, 653 (1984).
- ⁴⁵ G. E. Busch and K. R. Wilson, *J. Chem. Phys.* **56**, 3626 (1972).
- ⁴⁶ J. P. Simons and P. W. Tasker, *Mol. Phys.* **27**, 1691 (1974).
- ⁴⁷ The equation used to calculate the range of possible impact parameters for a given J state of CO with rotational energy E_{rot} is as follows:

$$m_a(m_\beta + m_\gamma)^2(E_{\text{avl}} - E_{\text{int,H}_2} - E_{\text{rot}})b^2/m_\beta m_\gamma(m_a + m_\beta + m_\gamma)r_{\beta\gamma}^2 \\ \pm [2(m_\beta + m_\gamma)(E_{\text{avl}} - E_{\text{int,H}_2} - E_{\text{rot}})/(m_a + m_\beta + m_\gamma)m_a]^{1/2} \\ \times (hJ_a m_a(m_\beta + m_\gamma)b/2\pi m_\beta m_\gamma r_{\beta\gamma}^2 \\ + h^2 J_a^2(m_\beta + m_\gamma)/4\pi m_\beta m_\gamma r_{\beta\gamma}^2 - E_{\text{rot}} = 0,$$

where h is Planck's constant, J_a is the rotational quantum number of the hydrogen, and $E_{\text{int,H}_2}$ is the internal energy of the hydrogen fragment. The $-$ or $+$ sign before the second term refers to H₂ rotation in the same or in the opposite direction, respectively, as the direction of CO rotation.

⁴⁸ M. D. Morse and K. F. Freed, *J. Chem. Phys.* **74**, 4395 (1981).